Egypt. J. of Appl. Sci., 38 (1-2) 2023 *1-13*

EVALUATION OF THE ANTIBACTERIAL EFFICACY OF BIOSYNTHESIZED ZINC OXIDE NANOPARTICLES (ZnO NPs) BY *Streptomyces albus* STRAIN W12 AGAINST WASTEWATER-ASSOCIATED BACTERIA.

Wafy, K.R.[1*] ; Walaa S. Mohamed[1] and Sabha M. El-Sabbagh[2]

1-Central Laboratory for Environmental Quality Monitoring, National Water Research Center, El-kanater El-khairia, P.M.B 13621, Egypt

2-Department of Botany and Microbiology, Faculty of Sciences, University of Menoufia, Shibin El-kom, P.M.B 32511, Egypt

***E-mail-Karamwafy@yahoo.com**

ABSTRACT

The synthesis of nanostructured materials has gained significant interest due to their unique properties and applications in various fields. The biological approach of nanoparticle synthesis is cheaper and environmentally friendly compared to conventional chemical methods. This study aimed to synthesize Zinc oxide nanoparticles (ZnO NPs) using actinomycetes and evaluate their antimicrobial properties. The synthesized nanoparticles were characterized using various techniques (UV-Vis spectroscopy, Fourier transform-infrared spectroscopy, scanning electron microscopy, X-ray diffraction analysis, and Zeta potential analysis) and their antibacterial activity was tested using the well diffusion method against four different bacteria species. The transmission electron microscope showed that the average size of ZnO NPs was 20–38 nm, while X-ray diffraction and energy-dispersive X-ray spectroscopy confirmed the purity of the biosynthesized ZnO NPs. The biosynthesized ZnO NPs showed effective antibacterial activity against *E. coli* MTCC 739, *Pseudomonas aeruginosa* MTCC 2453, *Staphylococcus aureus* MTCC 96, and *Bacillus subtilis* MTCC 736. Thus, biosynthesized ZnO NPs have the potential to be stable and eco-friendly nanoparticles with antibacterial activities.

Key Words: Nanoparticle; Antibacterial activity; ZnO NPs; Synthesis.

INTRODUCTION

Nanotechnology has emerged as the most revolutionary technology of the twenty-first century, impacting all aspects of human life and encompassing nearly every field of research with ground-breaking breakthroughs **(Yarotski *et al.*, 2009).** Nanomaterials have received interest because of their unique physical and chemical features, such as increased surface area to volume ratio, and magnetic and optoelectronic capabilities when compared to its bulk equivalent **(Qiu *et al.*, 2018).**

Fabrication of nanoparticles with controlled size, shape, and crystalline nature is a major focus in chemistry and biomedical research because it is a promising candidate for a variety of applications such as medical, electrochemistry, sensors, catalysis, drug delivery, and trace element detection, among others **(Singh *et al.*, 2021)**.

Traditionally, numerous physical, chemical, and mechanical processes have been employed to create superior nanomaterials of varying morphology and size, which exhibited efficient relevance at the industrial and commercial levels **(Khan *et al.*, 2019)**. However, the exorbitant expense of specialized instruments, alongside the hazardous side effects of chemicals on the environment, shifted the researchers' focus to creating nanoparticles using eco-friendly ways to tackle health and environmental challenges **(Islam *et al.*, 2022)**. Nature supplied researchers with innovative ideas for the fabrication of nanoparticles using biological systems employing a bio-mimetic method **(Ahmed *et al.*, 2016).** According to scientific evidence, bacteria, fungi, yeast, and plant extracts were employed to produce ecologically friendly nanomaterials **(Gunalan *et al.*, 2012).** These bioinspired nanoparticles were discovered to be biocompatible, cost-effective, and efficient in biomedicine. Actinomycetes are gram-positive filamentous organisms found in soils **(Bhatti *et al.*, 2017).** They are highly studied organisms due to their soil-degrading abilities as well as their powerful supply of antibiotics.

The application of zinc oxide has been reported in several physical and optical processes, including wastewater treatment, food packaging, and antimicrobial agents **(Shaba *et al.*, 2021).** zinc nanoparticles are recognized as non-toxicoxic, and biocompatible particles **(Mirzaei and Darroudi, 2017)**. The biological method for the synthesis of zinc nanoparticles is advantageous as it is simple and retains intact antimicrobial activity. Depending on the nature of these particles, they have a vast potential for antimicrobial activity against pathogenic microorganisms. The biological synthesis of nanoparticles is a viable, cost-effective, and safe synthesis route according to biomedical applications, which confer potential and more functional properties. Thus, the objectives of this study were to synthesize ZnO NPs by actinomycetes isolated from soil and to screen the antibacterial activity of biosynthesized nanoparticles against wastewater-associated bacteria **(Slman, 2012).**

MATERIAL AND METHODS

- **Chemicals**

All of the chemicals used, including the $ZnSO_4.7H_2O$, NaOH, and starch agar mediam, were provided by Merck. Every solution is made

with deionized water. All glassware ware cleaned with double distilled water, dried for 2 hours in a 180 °C oven, and stored in a dry container.

- **Isolation of actinomycetes**

Heat treatment was performed on soil samples to isolate actinomycetes. Samples were put in an oven at 100 °C for 60 min. Serial dilutions were prepared from samples and one ml of dilution was inoculated in starch agar media and incubated for 5 days at 30 °C, the isolates were stored at 4 °C for the next studies **(Abd El-Motaleb *et al.*, 2020)**. Actinomycete isolates were inoculated in starch broth media and cultured on a shaker at 30°C for 5 days before being centrifuged at 4500 rpm for 30 minutes to remove the biomass. The supernatant was collected and utilized to synthesize zinc oxide nanoparticles in a reaction with zinc sulfate **(Eid *et al.*, 2020)**.

- **Biosynthesis of zinc oxide nanoparticles by actinomycetes**

To synthesize ZnO nanoparticles, 20 isolates of Actinomycetes were scanned. To make ZnO NPs, 50 mL of zinc sulfate (0.1 M) and sodium hydroxide solution (0.4 M) were combined in a 250 mL conical flask, and 50 mL of actinomycetes culture was added to the same flask. The flask was then shaken at 40 °C for 15 minutes to generate the ZnO NPs. The flask was then microwaved for 2 minutes before being allowed to cool for 1 hour. The nanoparticles would settle naturally. The emergence of white deposits on the flask's bottom would confirm the creation of ZnO nanoparticles. After that, the ZnO nanoparticles were rinsed with deionized water and centrifuged at 3000 rpm for 10 minutes. The centrifugation was repeated until the supernatant was clear. The pellet was gathered in a tiny plate and dried for 8 hours in a muffle furnace at 400 °C until it appeared completely dry. As a consequence, The ZnO NPs powder was generated **(Mishra *et al.*, 2013)**.

- **Characterization of ZnO nanoparticles**

UV-Vis spectroscopy

The excitation spectra of biologically synthesized ZnO nanoparticles were examined using UV-visible spectroscopy. It was measured with a Hach DR 3900 Spectrophotometer with a resolution of 1 nm. To confirm the reduction of nanoparticles, an absorbance spectra scan of 300-750 nm was performed on the Hitachi double-beam spectrophotometer for re-suspended nanoparticles in deionized water **(Dobrucka and Dugaszewska, 2016).**

X-ray diffraction analysis (XRD)

The production of ZnO NPs was validated and the crystal structure was discovered using an X-ray diffractometer (XRD, D8, Bruker, Germany) **(Kumari *et al.*, 2017)**.

Fourier transform-infrared spectroscopy (FTIR)

The binding effectiveness of ZnO nanoparticles was determined using FTIR. The FTIR spectrophotometer (Thermo Fisher Nicolet iS50 FTIR Spectrometer) can be used to extract structural information from its different vibrational modes. FTIR measurement was performed directly on dried ZnO nanoparticles powder. Based on the frequency of 400-4000 cm^{-1}, the scanned FTIR result was reported **(Rajivgandhi *et al.*, 2022).**

Zeta potential analysis

The ZnO nanoparticles were re-suspended in a water solution and filtered using a 0.22 mm syringe filter. The dynamic light scattering approach was used to determine the size distribution of the nanoparticles. A zeta potential analyzer (Nano Brook Zeta PALS Potential Analyzer, Brookhaven) was used to scan the particle size, size distribution, and Zeta potential effect of ZnO NPs **(Rajivgandhi *et al.*, 2022)**.

Elemental dispersion analysis of X-Ray (EDAX)

The elemental composition of the synthesized ZnO nanoparticle was determined using EDAX. An X-ray diffractometer (XRD, D8, Bruker, Germany) was used to determine the presence or absence of ZnO NP confirmative peaks **(Kumari *et al.*, 2017)**.

Scanning electron microscopy (SEM)

Scanning electron microscopy (SEM, Quanta FEG 250) was used to determine the surface morphology of the nanoparticles. Zinc oxide nanoparticles were disseminated in 100% ethanol using ultrasonic agitation, then a portion of the solution was dropped onto a glass slide, and the solvent was evaporated at room temperature. The specimens were then coated with a thin gold coating by physical vapor deposition in a vacuum of roughly 3 mm thickness before being subjected to SEM examination **(Kumari *et al.*, 2017)**.

Transmission Electron Microscopy (TEM)

Transmission Electron Microscopy (TEM) analysis of synthesized silver and zinc oxide nanoparticles was prepared by drop-coating biosynthesized nanoparticles solution on carbon-coated copper TEM grids (400 μm × 40 μm mesh size). Samples were dried and kept under vacuum in desiccators before loading on to a specimen holder. TEM measurements were performed on a Tecnai- 12 (JEM-2100 electronic microscope, JEOL, Japan) electron microscope operated at an accelerating voltage of 120 kV **(Kumari *et al.*, 2017)**.

- **Identification of the actinomycetes isolates by 16S rRNA**

16S rRNA sequencing analysis identified the actinomycetes isolate responsible for the creation of ZnO nanoparticles. The isolate was inoculated in starch broth and incubated for 7 days at 28 °C. Quick-DNA Miniprep Plus Kit (Zymo Research Corp., USA) was used to extract genomic DNA. The polymerase chain reaction (PCR) method was

employed to amplify the 16S rRNA universal primers gene fragment using pure genomic DNA as a template. As primers, forward primer (5′ CACACTGGGACTGAGACACG 3′) and reverse primer (5′ TAGTTAGCCGGCTTCTTC 3′) were utilized. The following conditions were used for the PCR reaction: initial denaturation at 94°C for 6 minutes, 35 amplification cycles at 94°C for 45 seconds, annealing at 56°C for 45 seconds, 72°C for 1 minute, and final extension at 72°C for 5 minutes. UV fluorescence was employed to detect PCR amplification using agarose gel electrophoresis. The PCR product was sequenced using an automated sequencer and the identical primers mentioned previously. Using the NCBI BLAST provided at https://www.ncbi.nlm.nih.gov/nuccore/OQ255755, the 16S rRNA sequence was evaluated for similarity with the reference species included in the genomic database banks. Using MEGA version 6, the phylogenetic analysis of the sequence with the closely similar sequence of BLAST results was done **(Park *et al.*, 2019 and Ferrandis-Vila *et al.*, 2022)**.

- **Antibacterial activity using well diffusion method against some bacteria**

The antibacterial activity of ZnO nanoparticles synthesised with *Streptomyces al*bus strain w12 was tested using the agar well diffusion method against various reference bacterial strains (*E. coli* MTCC 739, *Pseudomonas aeruginosa* MTCC 2453, S*taphylococcus aureus* MTCC 96, and *Bacillus subtilis* MTCC 736). Bacterial cultures were cultivated overnight on nutrient agar media at 37 degrees Celsius before being injected into nutrient agar plates. The well was loaded with varied concentrations of ZnO nanoparticles (10, 25, and 50 g/mL), ceftriaxone was utilized as a positive control, and distilled water was used as a negative control. The plates were incubated at 37 degrees Celsius for 24 hours before measuring the zone of inhibition around the wells **(Dadi *et al.*, 2019 and Feroze *et al.*, 2020).**

RESULT AND DISCUSSION

- **Isolation of actinomycetes**

The current study used 20 isolates of actinomycetes species isolated from soil to synthesize ZnO nanoparticles. The isolated *streptomycetes albus* strain w12 was identified and proven as a synthesis of ZnO nanoparticles. The partly 16S rRNA sequences of strain w12 were matched with known representative Actinomycetes 16S rRNA sequences taken from the NCBI Gen Bank database. The partly 16S rRNA sequences of the w12 strain were also deposited in the Gen Bank database under the accession numbers: OQ255755.1 (Fig.1) **(Leblond-Bourget *et al.*, 1996 and Aydin *et al.*, 2021).**

Fig 1: Phylogenetic dendrogram produced using the neighbor-joining approach based on 16S rRNA gene sequence analysis, displaying the phylogenetic position of *Streptomyces albus* strain w12 OQ255755.1.

- **Characterization of ZnO nanoparticles**

The maximum absorption peak (λmax) of the synthesized ZnONPs measured using a UV-Vis spectrophotometer was at 322 nm (Fig. 2A), which agrees with the range of ZnO NPs analysis, demonstrating the presence of ZnO NPs in the colloidal solution **(Aminuzzaman *et al.*, 2018)**. Several research has reported comparable λmax values as approved for the successful manufacture of ZnO NPs **(Sarillana *et al.*, 2021)**.

The FTIR profiles of both the precipitated ZnO NPs before calcination and the calcinated ZnO NPs were shown in Fig. 2B to determine the presence or absence of distinct vibrational modes in the wavenumber range of 4000-400 cm^{-1}. In general, metal oxides produce absorption bands in the fingerprint section, notably below 1000 cm^{-1} as a result of interatomic vibrations **(Fiore and Pellerito, 2021)**. The peaks at 442 and 466 cm^{-1} relate to metal-oxygen interactions (ZnO stretching bonds), while the absorption peak at 874 cm^{-1} is caused by Zn tetrahedral coordination **(Lakshminarayana *et al.*, 2018)**. The apparent peaks at 1624 and 1418 cm^{-1} represent C=O stretching of aldehydes and carboxylic acids, respectively, and C-O stretching. The absorption peaks between 2800 and 3000 cm^{-1} correlate to C-H stretching vibrations **(Hadjiivanov *et al.*, 2020)**. Both spectra have a wide absorption peak at 3418 cm^{-1}, which may be connected to the vibrational mode of hydroxyl groups **(Ivashchenko *et al.*, 2016)**. Impurities may cause some unresolved bands in the precipitate. As a result, the FTIR data indicated the presence of ZnO NP biosynthesis.

The surface charge of ZnO NPs was evaluated using zeta potential analysis, which provides further information on their colloidal stability **(Rajivgandhi *et al.*, 2022)**. Fig 2C depicted the measured zeta potential of biosynthesized ZnO NPs in aqueous dispersion. Because of their strong negative zeta potential value (-18.1 mV), ZnO NPs had remarkable colloidal stability in an aqueous solution, avoiding agglomeration or aggregation for a lengthy period of time. This consistency is appealing for biological and environmental applications. Furthermore, the specific surface area of biosynthesized ZnO NPs was 6.2 m^2/g, which was comparable to that of some commercial ZnO NPs.

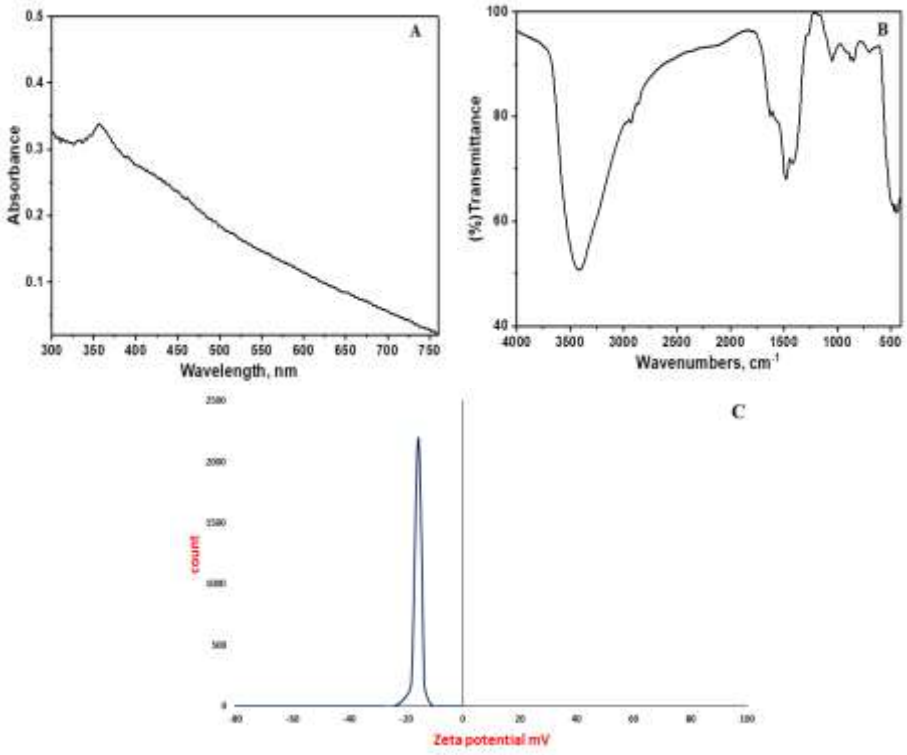

Fig 2: UV absorption spectra (a), FTIR analysis (b), and Zeta potential (c) of biological synthesized ZnO NPs

The morphology and particle size of biosynthesized ZnO NPs were examined using SEM and TEM. From the SEM micrograph (Fig: 3A), it was evident that the shape of ZnO NPs was almost spherical and uniform. In addition, the prepared ZnO NPs had less tendency to agglomerate, indicating a high surface area (active sites) which tended to improve the photocatalytic reactions. Furthermore, EDAX analysis was performed to investigate the topographies of the biosynthesized ZnONPs.

As illustrated in Fig: 3B, the recorded peaks at 1.03 and 8.63 KeV confirmed the presence of the Zn atom, where the apparent peak at 0.52 KeV represented the O atom, which was the main component of the ZnO NPs sample **(Barzinjy and Azeez, 2020)**. The elemental analysis revealed that the biosynthesized sample is in its highest purified form, and no traces of impurities were detected.

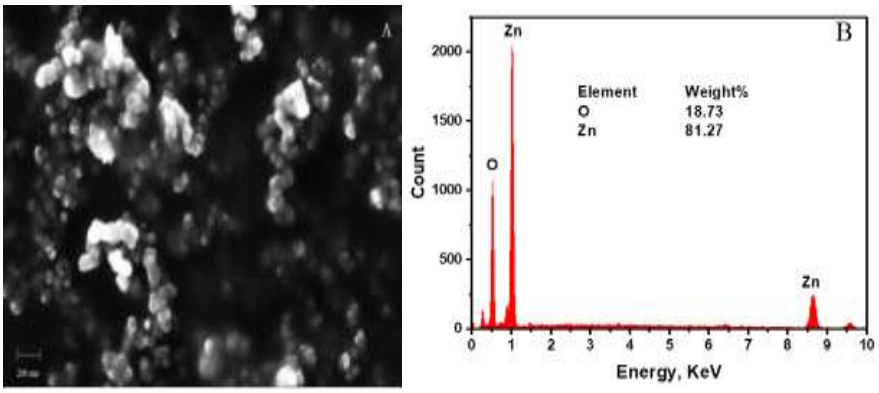

Fig 3: Morphological observation of SEM (A) and EDAX (B) of biological synthesized ZnO NPs

The diameter of the biosynthesized ZnO NPs ranges between 20 and 38 nm, as shown in Fig. 4B. XRD patterns were also acquired to have a better understanding of the phases and microstructure of the biosynthesized ZnO NPs. As shown in Fig: 4A, the obtained peaks corresponding to the (100), (002), (101), (102), (110), (103), (200), (112), and (201) planes, respectively, confirm the pure hexagonal wurtzite phase of ZnO NPs. The biosynthesized ZnO NPs were in their pure phase, free of contaminants, according to XRD measurements.

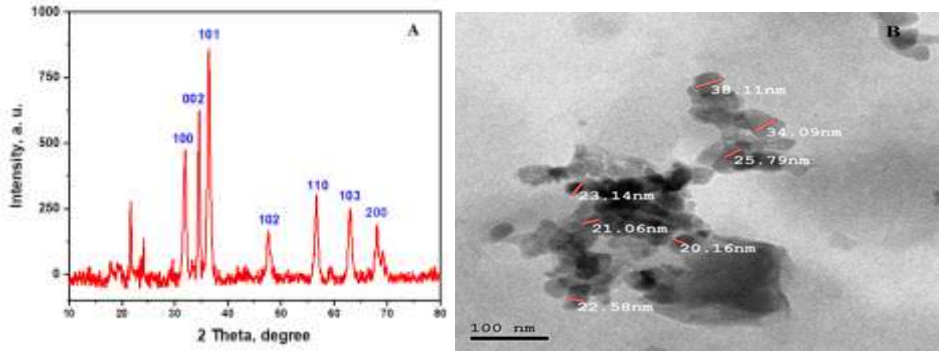

Fig 4. XRD (A) and TEM(B) analysis of biological synthesized ZnO NPs

- **Antibacterial activity using well diffusion method**

The antibacterial activity of produced ZnO nanoparticles on various bacteria was investigated in this study (*E. coli* MTCC 739, *Pseudomonas aeruginosa* MTCC 2453, *Staphylococcus aureus* MTCC 96, *Bacillus subtilis* MTCC 736). Using agar well diffusion assy (Fig 5& Table:1) ZnO nanoparticles includes inhibition zone against four bacteria species (*E. coli* MTCC 739, *Pseudomonas aeruginosa* MTCC 2453, *Staphylococcus aureus* MTCC 96, *Bacillus subtilis* MTCC 736) inhibition zone increase proportionally with increase ov zno concentration. Because of the nanoparticles' broad range of application potential, ZnO-NPs have been extensively studied for antibacterial activity. **El-Kattan, (2022)** discovered that ZnO-NPs had antibacterial action against both Gram-positive and Gram-negative bacteria **(El-Kattan *et al.*, 2022)**. Another study, **Pillai *et al.*, (2020)**, found that the antibacterial activity of green synthesized ZnO rised proportionally with the concentration of NPs **(Pillai *et al.*, 2020)**.

Fig 5. Antibacterial activity of biosynthesized ZnO NPs (A: 10 µg/ml, B: 25 µg/ml, C: 50 µg/ml, D: ceftriaxone 10 µg/ml, and E: distilled water).

Table.1: Diameter of inhibition zone of ZnO NPs against different microorganisms

Microorganism	Zone of Inhibition, mm			
	Ceftriaxone (10 µg/mL)	AgNPs		
		10 (µg/mL)	25 (µg/mL)	50 (µg/mL)
E. coli	**20.9 ± 1.9**	**12.0 ± 0.89**	**14.5 ± 1.67**	**18.0 ± 2.02**
P. aeruginosa	**19.7 ± 1.07**	**11.8 ± 1.84**	**13.5 ± 1.21**	**15.5 ± 1.55**
S. aureus	**17.6 ± 1.63**	**10.5 ± 1.02**	**12.5 ± 1.93**	**14.0 ± 1.5**
B. subtilis	**18.5 ± 1.65**	**10.9 ± 1.4**	**13 ± 1.09**	**14.9 ± 1.33**

The antibacterial activity of the synthesized ZnO NPs against *E. coli*, *P. aeruginosa* (Gram-negative bacteria) was higher than that of *S. aureus* and *B. subtilis* (Gram-positive bacteria) in the current study. The release of diffusible inhibitory chemicals from ZnO NPs caused bacterial group inhibition around the well.

CONCLUSION

The current study used a rapid, simple, and environmentally benign method to create zinc oxide nanoparticles and assess their efficiency against some dangerous bacteria. A particular isolate was isolated, and the zinc nanoparticles were synthesized using its supernatant. Several methods were utilized to analyse their qualities, and it was discovered that they were effective against a variety of bacteria. More research is needed to investigate their potential usage in water purification.

REFERENCE

Abd El-Motaleb, M. ; S. El-Sabbagh ; W. Mohamed and K. Wafy (2020). Biosorption of Cu^{2+}, Pb^{2+} and Cd^{2+} from wastewater by dead biomass of *Streptomyces cyaneus* Kw42. Int. J. Curr. Microbiol. Appl. Sci, 9, 422-435.

Ahmed, S. ; M. Ahmad ; B.L. Swami, and S. Ikram (2016). A review on plants extract mediated synthesis of silver nanoparticles for antimicrobial applications: A green expertise. J. Adv. Res., 7(1): 17-28.

Aminuzzaman, M. ; L.P. Ying ; W.S. Goh and A. Watanabe (2018). Green synthesis of zinc oxide nanoparticles using aqueous extract of *Garcinia mangostana* fruit pericarp and their photocatalytic activity. Bulletin of Materials Sci., 41: 1-10.

Aydin, F. ; S. Abay ; T. Kayman ; E. Karakaya ; H.K. Mustak ; I.B. Mustak and O. Guran (2021). *Campylobacter anatolicus* sp. nov., a novel member of the genus Campylobacter isolated from feces of Anatolian Ground Squirrel (*Spermophilus xanthoprymnus*) in Turkey. Systematic and Applied Microbiology, 44(6), 126265.

Barzinjy, A.A. and H.H. Azeez (2020). Green synthesis and characterization of zinc oxide nanoparticles using *Eucalyptus globulus* Labill. leaf extract and zinc nitrate hexahydrate salt. SN Appl. Sci., 2(5): 991.

Bhatti, A.A. ; S. Haq and R.A. Bhat (2017). Actinomycetes benefaction role in soil and plant health. Microbial Pathogenesis, 111: 458-467.

Dadi, R. ; R. Azouani ; M. Traore ; C. Mielcarek and A. Kanaev (2019). Antibacterial activity of ZnO and CuO nanoparticles against Gram positive and Gram negative strains. Materials Sci. and Engin. C, 104: 109968.

Dobrucka, R. and J. Długaszewska (2016). Biosynthesis and antibacterial activity of ZnO nanoparticles using *Trifolium pratense* flower extract. Saudi J. Biol. Sci., 23(4): 517-523.

Eid, A.M. ; A. Fouda ; G. Niedbała ; S.E.D. Hassan ; S.S. Salem ; A.M. Abdo and T.I. Shaheen (2020). Endophytic *Streptomyces laurentii* mediated green synthesis of Ag-NPs with antibacterial and anticancer properties for developing functional textile fabric properties. Antibiotics, 9(10): 641.

El-Kattan, N. ; A.N. Emam ; A.S. Mansour ; M.A. Ibrahim ; A.B. Abd El-Razik ; K.A. Allam, and S.A. Ibrahim, (2022). Curcumin assisted green synthesis of silver and zinc oxide nanostructures and their antibacterial activity against some clinical pathogenic multi-drug resistant bacteria. RSC Advances, 12(28): 18022-18038.

Feroze, N. ; B. Arshad ; M. Younas ; M.I. Afridi ; S. Saqib and A. Ayaz (2020). Fungal mediated synthesis of silver nanoparticles and evaluation of antibacterial activity. Microscopy Res. and Technique, 83(1): 72-80.

Ferrandis-Vila, M. ; S.K. Tiwari ; S. Mamerow ; T. Semmler ; C. Menge and C. Berens (2022). Using unique ORFan genes as strain-specific identifiers for *Escherichia coli*. BMC Microbiol., 22(1): 1-14.

Fiore, T., and Pellerito, C. (2021). Infrared Absorption Spectroscopy. Spectroscopy for Materials Characterization, 129-167.

Gunalan, S. ; R. Sivaraj and V. Rajendran (2012). Green synthesized ZnO nanoparticles against bacterial and fungal pathogens. Progress in Natural Science: Materials International, 22(6): 693-700.

Hadjiivanov, K.I. ; D.A. Panayotov ; M.Y. Mihaylov ; E.Z. Ivanova ; K.K. Chakarova ; S.M. Andonova and N.L. Drenchev (2020). Power of infrared and raman spectroscopies to characterize metal-organic frameworks and investigate their interaction with guest molecules. Chem. Rev., 121(3): 1286-1424.

Islam, F. ; S. Shohag ; M.J. Uddin ; M.R. Islam ; M.H. Nafady ; A. Akter and S.Cavalu (2022). Exploring the journey of zinc oxide nanoparticles (ZnO-NPs) toward biomedical applications. Materials, 15(6): 2160.

Ivashchenko, O. ; J. Jurga-Stopa ; E. Coy ; B. Peplinska ; Z. Pietralik and S. Jurga (2016). Fourier transform infrared and Raman spectroscopy studies on magnetite/Ag/antibiotic nanocomposites. Appl. Surface Sci., 364: 400-409.

Khan, I. ; K. Saeed and I. Khan (2019). Nanoparticles: Properties, applications and toxicities. Arabian J. Chem., 12(7): 908-931.

Kumari, R. ; M. Barsainya and D.P. Singh (2017). Biogenic synthesis of silver nanoparticle by using secondary metabolites from

Pseudomonas aeruginosa DM1 and its anti-algal effect on Chlorella vulgaris and Chlorella pyrenoidosa. Environ. Sci. and Poll. Res., 24: 4645-4654.

Lakshminarayana, G. ; K.M. Kaky ; S. Baki ; A. Lira ; A. Meza-Rocha ; C. Falcony and A. Abas (2018). Nd^{3+}-doped heavy metal oxide based multicomponent borate glasses for 1.06 μm solid-state NIR laser and O-band optical amplification applications. Optical Materials, 78: 142-159.

Leblond-Bourget, N. ; H. Philippe ; I. Mangin and B. Decaris (1996). 16S rRNA and 16S to 23S internal transcribed spacer sequence analyses reveal inter-and intraspecific *Bifidobacterium phylogeny*. Int. J. Systematic and Evolutionary Microbiol., 46(1): 102-111.

Mirzaei, H. and M. Darroudi (2017). Zinc oxide nanoparticles: Biological synthesis and biomedical applications. Ceramics Int., 43(1): 907-914.

Mishra, M. ; J.S. Paliwal ; S.K. Singh ; E. Selvarajan ; C. Subathradevi and Mohanasrinivasan, V. (2013). Studies on the inhibitory activity of biologically synthesized and characterized zinc oxide nanoparticles using *Lactobacillus sporogens* against Staphylococcus aureus. J. Pure. Appl. Microbiol., 7(2): 1263-1268.

Park, J. ; Y. Kim ; H. Xi ; Y.J. Oh ; K.M. Hahm and J. Ko (2019). The complete chloroplast genome of common camellia tree, Camellia japonica L.(Theaceae), adapted to cold environment in Korea. Mitochondrial DNA Part B, 4(1): 1038-1040.

Pillai, A.M. ; V.S. Sivasankarapillai ; A. Rahdar ; J. Joseph ; F. Sadeghfar ; K. Rajesh and G.Z. Kyzas (2020). Green synthesis and characterization of zinc oxide nanoparticles with antibacterial and antifungal activity. J. Molecular Structure, 1211: 128107.

Qiu, M. ; W.X. Ren ; T. Jeong ; M. Won ; G.Y. Park ; D.K. Sang and J.S. Kim (2018). Omnipotent phosphorene: a next-generation, two-dimensional nanoplatform for multidisciplinary biomedical applications. Chem. Soc. Rev., 47(15): 5588-5601.

Rajivgandhi, G. ; B.M. Gnanamangai ; T.H. Prabha ; S. Poornima ; M. Maruthupandy ; N.S. Alharbi and W.J. Li (2022). Biosynthesized zinc oxide nanoparticles (ZnO NPs) using actinomycetes enhance the anti-bacterial efficacy against *K. Pneumoniae*. J. King Saud Uni. Sci., 34(1): 101731.

Sarillana, Z. ; E. Fundador, and N. Fundador (2021). Synthesis of ZnO nanoparticles using *Theobroma cacao* L. pod husks, and their antibacterial activities against foodborne pathogens. Int. Food Res. J., *28*(1).

Shaba, E.Y. ; J.O. Jacob ; J.O. Tijani and M.A.T. Suleiman (2021). A critical review of synthesis parameters affecting the properties of

zinc oxide nanoparticle and its application in wastewater treatment. Appl. Water Sci., 11: 1-41.

Singh, K.R. ; V. Nayak ; J. Singh ; A.K. Singh and R.P. Singh (2021). Potentialities of bioinspired metal and metal oxide nanoparticles in biomedical sciences. RSC Advances, 11(40): 24722-24746.

Slman, A.A. (2012). Antibacterial activity of Zno nanoparticle on some Gram-positive and Gram-negative bacteria. Iraqi J. Physics, 10(18): 5-10.

Yarotski, D.A. ; S.V. Kilina ; A.A. Talin ; S. Tretiak ; O.V. Prezhdo ; A.V. Balatsky and A.J. Taylor (2009). Scanning tunneling microscopy of DNA-wrapped carbon nanotubes. Nano Letters, 9(1): 12-17.

تقييم الفعالية المضادة للبكتيريا للجسيمات النانومترية لأكسيد الزنك المخلقة بيولوجيًا عن طريق الاستربتوميسس البس سلالة W12 ضد البكتيريا المرتبطة بمياه الصرف الصحي.

كرم ربيع وافى[1] ، ولاء صلاح الدين محمد[1] ، صابحة محمود الصباغ

1–المعامل المركزية للرصد البيئى – المركز القومى لبحوث المياة القناطر الخيرية ، ص 13621 ، مصر

2– قسم النبات و الميكروبيولوجى– كلية العلوم– جامعة المنوفية شبين الكوم ، P.M.B 32511 ، مصر

يجذب تخليق المواد النانومترية اهتمامًا كبيرًا نظرًا لخصائصها الفريدة وتطبيقاتها في مختلف المجالات الحديثة. يُعد الأسلوب الحيوي لتخليق الجسيمات النانومترية أرخص وأكثر صداقه للبيئة مقارنةً بالأساليب الكيميائية التقليدية. هدفت هذه الدراسة إلى تخليق جسيمات أكسيد الزنك النانومترية باستخدام الاكتينوميسيتات وتقييم خصائصها المضادة للميكروبات. تم توصيف الجسيمات المركبة باستخدام تقنيات مختلفة (طيف الأشعة فوق البنفسجية المرئية و طيف الأشعة تحت الحمراء و المجهر الإلكتروني الماسح و تحليل انبعاثات الأشعة السينية وتحليل الزيتا بوتنشيال) ، كما تم اختبار نشاطها المضاد لبعض انواع البكتيريا و أظهر المجهر الإلكتروني الحجم المتوسط لأكاسيد الزنك النانومترية بينما أكد تحليل الأشعة السينية وتحليل الأشعة السينية المنتثية الطاقة نقاء اكاسيد الزنك النانومترية بالأسلوب الحيوي. أظهرت سلالة *Streptomyces albus* w12 OQ255755.1 نشاطًا مضادًا فعالًا ضد *E. coli* MTCC 739، *Pseudomonas aeruginosa* MTCC 2453، *Staphylococcus aureus* MTCC 96 ، و *Bacillus subtilis* MTCC 736. وبالتالي ، تمتلك جزيئات الزنك النانومترية المخلقة حيويا بواسطة الاكتينوميسيتات الإمكانات اللازمة لأن تكون جسيماتً ذات استقرارية وصديقة للبيئة وذات فعالية مضادة للبكتيريا الموجبة والسالبة لصبغة جرام.